*International Journal of Engineering Applied Sciences and Technology, 2024*
**Vol. 9, Issue 06, ISSN No. 2455-2143, Pages 14-24**
**Published Online October 2024 in IJEAST (http://www.ijeast.com)**

# ADAPTIVE RULE BASE FUZZY LOGIC LOAD FREQUENCY CONTROL IN TWO AREA POWER SYSTEM

Maruwan A Adrees, Moneer A Faraj
Department of Electrical and Electronics Engineering,
Omar Al-Mukhtar University, Al Baida, Libya

Tawfiq H. Elmenfy
Department of Electrical and Electronic Engineering,
University of Benghazi, Benghazi, Libya

Shukri Ali
[3]Asalam International University,
benghazi, Libya

*Abstract:* **In this paper, the adaptation to rule bases of the designed fuzzy logic load frequency controller (ARFLFC) for interconnected two-area power system load frequency control is designed as a decentralized controller. The proposed ARFLFC controller has been designed to damp the frequency and the tie line power flow oscillations and to track its error to zero at steady state under a sudden load disturbance in the power area. The main advantage of the proposed controller is that it can handle the nonlinearities and uncertainties of the system. The controller parameters are updated online, utilizing both the frequency and the tie-line power deviations as adaptation signals. Time-domain simulations have been performed using MATALB/ SIMULINK to show the efficiency of the proposed ARFLFC A bench-mark problem of a two area power system is used to demonstrate the performance of the proposed AFLFC controller and to show its superiority over conventional integral controller. The results illustrate that, in comparison to integral control, the proposed AFLFC minimizes the interchanged tie power, provides effective damping, and minimizes the overshoot of frequency deviations.**

*Keywords:* **Load Frequency Control, Multi-Area Power System and Adaptive Fuzzy Logic controller**

## I. INTRODUCTION

A Power system is a complicated, nonlinear system where many generating units are interconnected to respond to changes in power demand and power generation. To make the power system balanced, the utilities' tie-line power transmission lines must have a balanced system frequency. If there is a load disruption, it will affect any regions that are connected by tie lines [1]. One of the major issues of discussion in the power systems area at the moment is load frequency control. By using non-adaptive control methods like PID and classical fuzzy control, LFC aims to reduce frequency deviations and keep the scheduled power at the target value even when load disturbances vary throughout the interconnected control areas.

Over the past few decades, researchers have developed numerous strategies for load frequency control to guarantee that the tie-line power flow and system frequency stay at their scheduled values in the case of automated generation control issues. Most automatic generation control systems use conventional linear control, with fixed-gain PI controllers being the most often used technology, according to the literature study [2]. However, as the market for energy grows tremendously, improved control methods become necessary to ensure the smooth operation of many interconnected units. Typically, advanced tuning methods are incorporated into the control law derivation. In order to overcome the weaknesses of conventional PI controllers, The trial-and-error method has been investigated by many researchers to reduce the complexity of these techniques for tuning PID parameters. In reference [3], a trial-and-error approach has been used to obtain the parameters of a PI controller that is designed for three-area load frequency control. Additionally, the PID controller's reliability and simplicity of structure make it ideal for optimizing PID gains under different operating conditions. A three-area interconnected power system design that uses genetic algorithms to adjust the PID controller's parameters is described in reference [4]. The response's performance improved, results. The bioinspired algorithm was effective

*International Journal of Engineering Applied Sciences and Technology, 2024*
**Vol. 9, Issue 06, ISSN No. 2455-2143, Pages 14-24**
**Published Online October 2024 in IJEAST (http://www.ijeast.com)**

and efficient while implementing the AGC/LFC [5]. Cuckoo search, ant colony optimization, and practical swarm optimization (PSO) [6-8] are examples of optimization methods that can tune PID parameters to determine the minimum global optima. A high order differential feedback controller and a developed were proposed for LFC in multi-area power systems. The gains of these controllers were optimally tuned using PSO [9].

Most modern automatic generation control systems utilize advanced artificial intelligence-based controllers, including fuzzy logic controllers [10], sliding mode control [11], and artificial neural network controllers [12]. Fuzzy logic control has been proposed by many researchers as having the ability to adapt to changing conditions with quick decisions. The main advantage of FLC is that it can control systems that have difficulty obtaining mathematical models. In addition, it is used to overcome a system's nonlinearity and variations[13]. Fuzzy-logic control applications to power systems have been growing quickly lately, particularly in relation to load frequency control issues and power system stability issues [14]. Sharma and Yesil provided many adaptive fuzzy scheduling algorithms for PLD and/or traditional PI controllers. Although these techniques yield good results, the transient reactions of the system exhibit some oscillation [15, 16].

An optimal neural network (ANN) based LFC has been proposed to handle rapid load changes in power systems. Using particle swarm optimization to train the ANN, this controller achieves lower mean square error and improved frequency regulation. It has been shown to be more effective than conventional ANN and PID methods, particularly in multi-area power systems [17].

In this research, a fuzzy logic load frequency controller was developed that adapts its rule bases based on linguistic fuzzy basis functions. Two compensate for variations in tie-line power and system frequency drop when the step load input PL for each plant in the system varies [18].

## II. MODELLING OF SINGLE AREA POWER SYSTEM

The transfer function approach is utilized to produce the models of the governor, load, prime mover, and generator, which are then integrated to make a full block diagram of an isolated power.

### 2.1 Governor Model

$\Delta Pg$ is altered by a pressure-driven speaker to steam valve position $\Delta PV$. Tg is the senator's time consistency, while the representative's move capacity is provided in Equation 1 [19].

$$\frac{\Delta P_V(s)}{\Delta P_g(s)} = \frac{1}{1+Tgs} \qquad (1)$$

### 2.2 Prime Mover (turbine) Model

It is used to provide mechanical power; it might be steam for a steam turbine or a water divider for a pressure-driven turbine. Prime mover model in Equation. 2 links mechanical power $\Delta$ yield to change in steam valve $\Delta PV$ worth exchange capacity [19].

$$\frac{\Delta P_m(s)}{\Delta P_V(s)} = \frac{1}{1+Tts} \qquad (2)$$

### 2.3 Load and Inertia Model

It is sensitive to frequency variation and may be evaluated using the speed load trademark, as shown in Equation. 3 [19].

$$\frac{\Delta\omega(s)}{\Delta Pm - \Delta Pl} = \frac{1}{2H+D} \qquad (3)$$

The frequency bias factor (B) is the sum of the frequency-sensitive burden change (D) and the speed governor system (1/R) for the steam turbine, as indicated in Equation 4 [19].

$$B = \frac{1}{R} + D \qquad (4)$$

Equations 1 to 4 are used to demonstrate the system in Figure 1.

*International Journal of Engineering Applied Sciences and Technology, 2024*
**Vol. 9, Issue 06, ISSN No. 2455-2143, Pages 14-24**
**Published Online October 2024 in IJEAST (http://www.ijeast.com)**

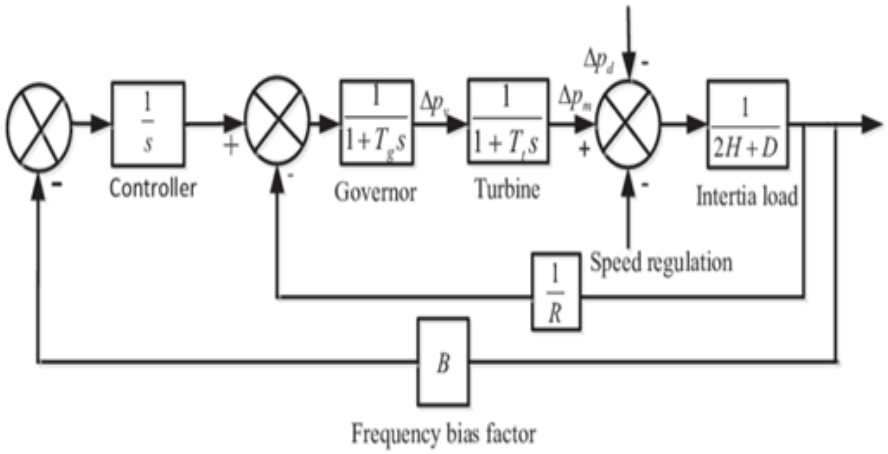


Figure 1: Single Area Power System with LFC

## III. MODEL OF OVERALL POWER SYSTEM WITH LOAD FREQUENCY CONTROL

The complete model of two parallel-connected power system plants is illustrated in Figure 2, which includes the governor-turbine system and the controller. All of the blocks in this model are usually nonlinear, time-variant, and/or non-minimum-phase systems [20]. A tie-line connects the two control areas. The disturbance load variations that affect the frequency in two areas as well as the frequency ties line power flow between the areas [21] are represented by $PL_1$, and the frequency changes in area 1 and area 2 are represented by $\Delta f_1$ and $\Delta f_2$, respectively. The proposed controllers have two control outputs: $U_1$, and $U_2$.

Due to parametric uncertainty, the power systems must have small oscillations in the transient frequency magnitude. To return each area's frequency and net tie line power to their nominal values, the Area Control Error (ACE) is utilized to lower its own value to zero, as indicated below:

$$ACE_1 = \Delta P_{12} + B_1 \Delta f_1 \quad (5)$$

$$ACE2 = \Delta P21 + B2\Delta f2 \quad (6)$$

Where ΔP12 and ΔP21 indicate changes in the tie line power plant, B1, B2, represent bias frequencies for each plant, and Δf1 and Δf2 represent frequency deviations for each plant.

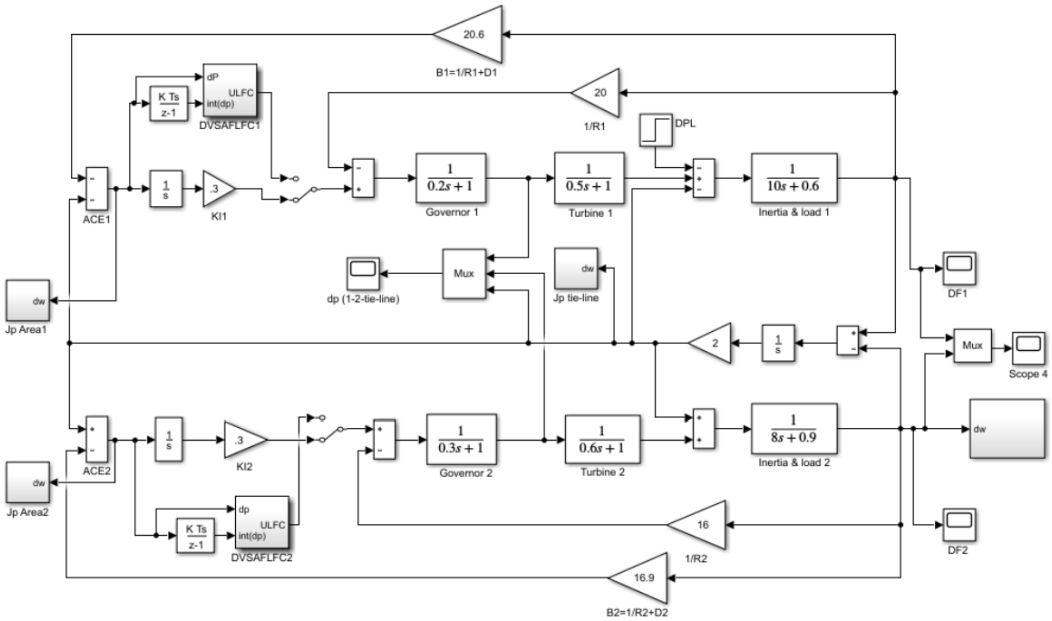


Figure2: Transfer function block diagram of two area power systems.

*International Journal of Engineering Applied Sciences and Technology, 2024*
**Vol. 9, Issue 06, ISSN No. 2455-2143, Pages 14-24**
**Published Online October 2024 in IJEAST (http://www.ijeast.com)**

## IV. STANDARD FUZZY LOGIC CONTROLLER

The main problem with nonadoptive control, such as conventional integral controllers and standard fuzzy control, is that their parameters' are fixed and don't adapt to changes in different operating points; they are tuned and designed for a particular operating point, which in our work is the disturbance load changes. As a result, the adaptive fuzzy controller proposed in this work has the ability to adjust its rule basis online [22]. Fuzzy logic control has been found to be a better replacement for integral control for load frequency control. Figure 4 illustrates the T-S fuzzy inference process, which consists of three parts: fuzzification of the input variable, evaluation and fuzzy rule inference, and finally defuzzification. The fuzzifer includes two input values and translates them into truth values (fuzzy variables) using seven membership functions for each input and input gain. The seven triangle membership functions for seven linguistic variables have been used to represent the fuzzy sets variable from big negative to big positive (NB, NM, NS, Z, PS, PM, PB) at centroids (−1, −0.667, −0.333, 0, 0.333, 0.667, 1), as seen in Figure 3.

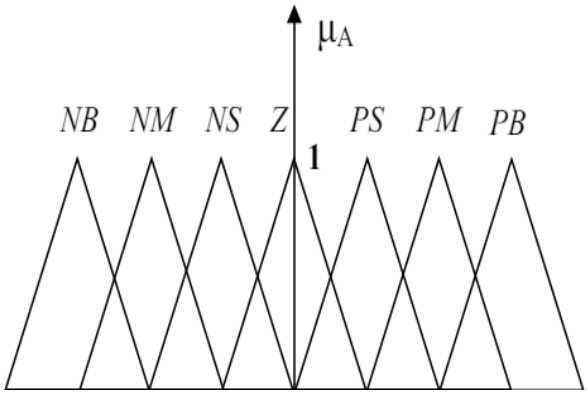


Figure 3: Fuzzy variable Xi with seven Membership function [23]

In this work, the power deviation and its integral as the controller input variables are fed to fuzzy LFC through input gains Ke and Kde, respectively.
In the second step, fuzzy rule inference is responsible for making the fuzzy decision based on defined fuzzy rules. Table 1 shows 49 rules using two controllers as the input and one output fuzzy set that is represented by their singletons. The scalar value ($\omega_i$) that represents the strength of the ith rule consequent is determined by reading the 'and' conjunction as a product of the membership values.

Table 1. Fuzzy-logic LFC rules

| | $\Delta P$ | | | | | | |
|---|---|---|---|---|---|---|---|
| $\Delta \dot{P}$ | NB | NM | NS | Z | PS | PM | PB |
| NB | NB | NB | NB | NB | NM | NS | Z |
| NM | NB | NB | NM | NM | NS | Z | PS |
| NS | NB | NM | NM | NS | Z | PS | PM |
| Z | NM | NM | NS | Z | PS | PM | PM |
| PS | NM | NS | Z | PS | PM | PM | PB |
| PM | NS | Z | PS | PM | PM | PB | PB |
| PB | Z | PS | PM | PB | PB | PB | PB |

The defuzzification stage, which is predicated on the T-S defuzzification, includes the third part.

$$U_f = \frac{\sum_{i=1}^{M} \omega_i \theta_i}{\sum_{i}^{M} \omega_i} = \underline{\theta}^T \underline{\zeta} \qquad (7)$$

where $\zeta = [\zeta_1 \dots \zeta_i \dots \zeta_M]^T$, $\zeta_i = \frac{\omega_i}{\sum_{k=1}^{M} \omega_k}$, and

$\theta_T$=[$\theta_1 \dots \theta_M$]. and $\theta_i$ is the $i_{th}$ output fuzzy singleton. In a standard fuzzy system, the values ,…,$\theta_M$ are fixed after they are set once. This paper's major contribution is the computation-efficient approach that is suggested to adjust $\theta_1$,…, $\theta_M$ online with the objective of improving the fuzzy FLC performance.

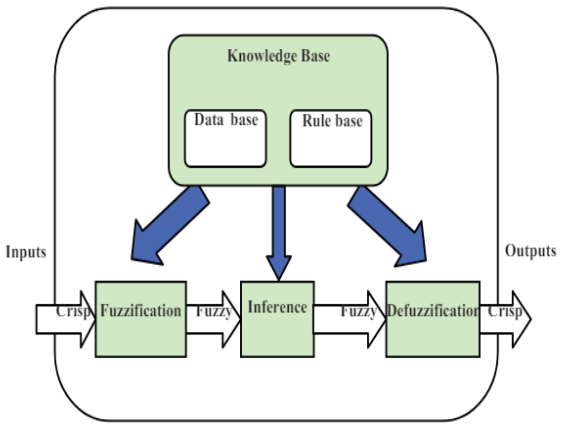


Figure 4: The basic structure of the fuzzy controller [24]

## V. ARFLFC ALGORITHM

Adaptive fuzzy control is a technique of adjusting a controller's parameters adaptively depending on feedback from the system by using fuzzy logic. Adaptive controllers

*International Journal of Engineering Applied Sciences and Technology, 2024*
**Vol. 9, Issue 06, ISSN No. 2455-2143, Pages 14-24**
**Published Online October 2024 in IJEAST (http://www.ijeast.com)**

differ from conventional controllers in that they have variable controller parameters that can be adjusted online in response to signals in the system. Nonlinear and unpredictable systems that are challenging to model or control with traditional techniques can be handled via direct adaptive systems.
It uses a fuzzy system to directly approximate the ideal controller without requiring a model of the system. Direct adaptive fuzzy has some advantages over other adaptive fuzzy approaches, including the ability to reduce the number of adaptive laws and the complexity of the controller structure. Furthermore, the tracking performance and robustness of the closed-loop system can be enhanced.

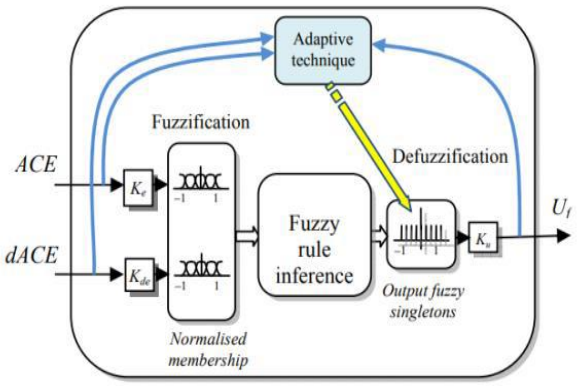


Figure 5: The structure of the proposed AFLFC [25]

The suggested ARFLFC's structure is shown in Fig. 5. Our ARFLFC is based on (7), where an adaptable approach is used to modify , $i$= 1,…,$M$ on-line. The centroids of the membership functions of the controller output are represented by the vector $\theta$. The fuzzy singletons in the controller output are represented by the vector θ, as shown in Table 2, there will be nine rules for each of the three fuzzy subsets in systems with two inputs.
When $\theta_i$ is tuned, all rules that use the output fuzzy set with the centeroid $\theta_i$ change. The proposed ARFLFC uses fewer rules than the standard fuzzy logic because of this dynamic rule adjustment. Compared to other adaptive systems, the variable structure feature significantly reduces the computational effort [26]. The suggested controller's implementation is straight-forward. The centeroids ,=1,…,$M$ are first computed. After that, Eq. (7) is used.
Now consider a $n$th-order nonlinear system of the form:

$$y^{(n)} = f(\underline{x}) + b(u) \qquad (8)$$

Where the $y \epsilon R$ is the output of system and $u \epsilon R$ is the input of the system while (·) and b represent an unknown real nonlinear function and an unknown constant, respectively.
$X = [x,,\ldots,_{(n-1)}]^T \epsilon R_n$ is the system state vector, and $y_{(n)}$ is the $r_{th}$ derivative of $y$ . The output y must track a reference signal $y_m$, which is chosen so that its derivatives up to the $n_{th}$ order are exited. The tracking error can be defined as follows:

$$e = ym - y,= \dot{y}m - y,e(n)= ym(n) - y(n) \qquad (9)$$

Thus, it is possible to choose the tracking error state vector, $e$, as $e=[e\ \dot{e}\ \ldots\ e_{n-1}]^T$
The feedback control law can be written as follows if $(X)$ and $b$ are known:

$$u = \frac{1}{b}[-f(\underline{x}) + y_m^{(n)} + \underline{K}^T \underline{e}] \qquad (10)$$

where the design vector $K$ is given by $K_T = [K_n\ K_{n-1}\ \ldots\ K_1]$
Substituting (10) into (8) leads to

$$y^{(n)} = y_m^{(n)} + \underline{K}T^T\ \underline{e} \qquad (11)$$

can be rewritten as follows in accordance with the definition of the tracking error (11) in (9):

$$e^{(n)} + \underline{K}^T\ \underline{e} = e^{(n)} + K_1 e^{(n-1)} + \\ +K_n e = 0 \qquad (12)$$

The error model's characteristic equation (12) can be written as follows:

$$S^n + K_1 S^{n-1} + \cdots .. + K_n = \\ 0 \qquad (13)$$

To ensure stability, the parameters $K_{1,2},\ldots,K_n$ are chosen so that the roots of (13) are on the left side of the s-plane. It is not possible to apply the control law (10) since $(x)$ $and$ $b$ are unknown. According to the universal approximation theorems [27] and [28], $u$ can be approximated by a fuzzy system.Then it is possible to write.

$$u \approx \dot{\theta}^T\ \underline{P}(\underline{X}) \qquad (14)$$

In this case, the fuzzy basis function vector is denoted by $(X)$, and the estimated vector of the centeroids of the membership functions assigned to u is denoted by $\theta$. And certain choices need to for the three steps of fuzzy controller order to create such a relationship function [29].

$$\underline{P}(\underline{X}) = \frac{\prod_{i=1}^{p} \mu_{F_i^l}(x_i)}{\sum_{l=1}^{M} \prod_{i=1}^{p} \mu_{F_i^l}(x_i)} \qquad (15)$$

*International Journal of Engineering Applied Sciences and Technology, 2024*
**Vol. 9, Issue 06, ISSN No. 2455-2143, Pages 14-24**
**Published Online October 2024 in IJEAST (http://www.ijeast.com)**

Depending on an estimate value $\theta$ of the actual values , the control law (14) is applied. Thus, the control signal may be expressed as follows:

$$u = u_c(\underline{\theta}, \underline{x}) = \underline{\dot{\theta}}^T \underline{P(X)} \quad (16)$$

Substituting $(\theta,x)$ in (14) leads to

$$y^{(n)} = f(x)+bu_c(\theta,x) \quad (17)$$

Adding and subtracting $bu$ to (17) results:

$$^{(n)} = (x)+bu+b(u_c(\theta,x \quad (18)$$

The error model corresponding to the closed-loop system (18) may be demonstrated to be similar to the derivative of (11):

$$e^{(n)} = -\underline{K}^T \underline{e} + b\left(u - u_c(\underline{\theta}, \underline{x})\right) \quad (19)$$

The controlled canonical form of equation (19) may be obtained by selecting:

$$\begin{aligned} \dot{e}_1 &= \dot{e} = e_2, \\ \dot{e}_2 &= \ddot{e} = e_3, \\ &\vdots \\ \dot{e}_{n-1} &= e^{(n-1)} = e_n \\ \dot{e}_n &= e^{(n)} = -\underline{k}^T \underline{e} + b(u - u_c(\underline{\theta}, \underline{x})) \end{aligned} \quad (20)$$

Consequently, the state space model has resulted in the following form:

$$\underline{\dot{e}} = A_c \underline{e} + \underline{b_c}(u - u_c(\underline{\theta}, \underline{x})) \quad (21)$$

Where

$$A_c = \begin{bmatrix} 0 & 1 & 0 & \dots & 0 \\ 0 & 0 & 1 & \ddots & \vdots \\ 0 & \ddots & \ddots & \ddots & 0 \\ 0 & 0 & \dots & 0 & 1 \\ -K_n & -K_{n-1} & \dots & -K_2 & -K_1 \end{bmatrix}, \underline{b_c} = \begin{bmatrix} 0 \\ 0 \\ \vdots \\ 0 \\ b \end{bmatrix}$$

The eigenvalues of $A_c$ are placed in a predetermined region on the left side of the s-plane by selecting the design parameters $K_{1,2,\dots,}k_n$. Typically, the second Lyapunov approach is used to determine the estimate value, $\theta$, which guarantees the stability of the adaptive system. To show that, consider the next Lyapunov function.

$$V = \frac{1}{2} \underline{e}^T p \underline{e} + \frac{b}{2} \underline{\emptyset}^T \Gamma^{-1} \underline{\emptyset} \quad (22)$$

V is the time derivation while $\emptyset=\theta-\theta$ is the error estimate and P and $\Gamma$ are positive definite matrices. The results of $P$ and $\emptyset$ computations are shown below. As seen below, $\Gamma$ is normally taken into consideration in the design as a diagonal matrix.

$$\dot{V} = \frac{1}{2}\left(\underline{e}^T P \underline{\dot{e}} + \underline{\dot{e}}^T P \underline{e}\right) + b \underline{\emptyset}^T \Gamma^{-1} \underline{\dot{\emptyset}} \quad (23)$$

Substituting for $\dot{e}$ from (21) into (23) leads to

$$\dot{V} = \frac{1}{2}(\underline{e}^T P A_c \underline{e} + \underline{e}^T P \underline{b_c} \emptyset^T \underline{P(X)} + \underline{e}^T A_c^T P \underline{e} + \underline{b}^T P \underline{e} \underline{\emptyset}^T \underline{P(X)}) + b \underline{\emptyset}^T \Gamma^{-1} \underline{\dot{\emptyset}} \quad (24)$$

Equation (24) can be simplified to (25)

$$\dot{V} = \underline{e}^T (P A_c + A_c^T P) \underline{e} + \emptyset^T \underline{P(X)} \underline{b_c}^T P \underline{e} + b \underline{\emptyset}^T \Gamma^{-1} \underline{\dot{\emptyset}} \quad (25)$$

If ($V$) is negative semidefinite, then the closed-loop system (21) is stable. The algebraic Lyapunov equation has a solution, $P$, since $A_c$ has stable eigenvalues:

$$P A_c + A_c^T P = -Q \quad (26)$$

Where Q is an arbitrary chosen positive semi-definite matrix. Use [29] as the adaptation law.

$$\underline{\dot{\emptyset}} = -\frac{1}{b} \underline{b_c}^T P_n \underline{e} \Gamma \underline{P(x)} \quad (27)$$

Where $P_n$ represents the matrix P's second column. As a result, (24) may be rewritten as:

$$V = -\frac{1}{2} \underline{e}^T Q e \quad (28)$$

The closed-loop system (21) is clearly stable if the adaptation law (27) is used, as shown by Eqn. 28. In order to perform equation (27) and compute $\theta$, it is necessary to suppose that $\theta$ is locally constant and that its variation is significantly slower than that of $\theta$ [30]. The estimate value $\theta$ is given by

$$\theta=1/b\ b_c^T Pn\ e\Gamma\ P(X) \quad (29$$

The adaptation gain Γ is represented by the diagonal matrix that the designer selects, with the ith diagonal member $\gamma_i$. The product $b_c{}^T P$ is equivalent to $bP_n$ where $P_n$ is the $n$th column of $P$, because of the special arrangement of the vector $b_c$. Due to the adoption of a pure integrator, the adaptation law (29) contains multiple drawbacks [30]. An estimator that is based on variable structures is developed in

*International Journal of Engineering Applied Sciences and Technology, 2024*
**Vol. 9, Issue 06, ISSN No. 2455-2143, Pages 14-24**
**Published Online October 2024 in IJEAST (http://www.ijeast.com)**

[31], beginning with the sigma-modification approach. For the efficient numerical implementation of our estimator, we chose to employ the variable structure approach since it produces robust performance. The *i*th estimate provided by (29) can be expressed as follows:

$$\dot{\theta}_i = \gamma_i \, \underline{e}^T \underline{P}_n \zeta_i(\underline{x}) \qquad (30)$$

The corresponding law of sigma-modification is [30].

$$\mu\dot{\theta}_i = \gamma_i \, \underline{e}^T \underline{P}_n \, \zeta_i \, (\underline{x}) - \sigma(\theta_i - \theta_i \, (0)) \qquad (31)$$

The design parameters consist of μ, and $\sigma$ constants. The initial estimate of $\theta_i$ is represented by (0). After choosing $\sigma$=1,μ→0 $and$ $\gamma_i = \theta_i / \|e_T P_n\| \zeta_i \, (x)$, we can rewrite (31) as

$$\theta_i = \overline{\theta}_i sgn(\underline{e}^T \underline{P}_n) + \theta_i(0) \qquad (32)$$

Where $\theta_i$ is a constant that the designer sets to indicate the range of possible variations in $\theta_i$ around (0). More confidence in the corresponding initially value (0) is reflected in a smaller $\theta_i(0)$. In (32), the sat(.) function commonly replaced replaced for the sgn(.) function to avoid chattering and guarantee a smooth variations of $\theta_i$, The estimator is therefore used as follows:

$$\theta_i = \overline{\theta}_i \, sat(\underline{e}^T \underline{P}_n) + \theta_i(0) \qquad (33)$$

In order to calculate $U_f$, the estimates produced by (33) are used.

$$U = u_c(\underline{\theta}, \underline{x}) = \underline{\hat{\theta}}^T \, \underline{P} \, (\underline{X}) \qquad (34)$$

## VI. THE DESIGN PROCEDURE FOR THE PROPOSED ARFLFC

A.Step 1

Let the inputs to the fuzzy basis function (FBF) be: $x_1$=Δ$P$ (power deviation), $x_2$=Δ$P$ (integral of power deviation), which means that:=[$x_1$ $x_2$ ]$_T$ = [ Δ$P$ Δ$P$ ]$_T$ . Given that the aim of the LFC controller is to reduce the deviation of the error (system frequency) to zero, it seems reasonable to select the power deviation Δ$P$ and its integrateΔ$P$ as input signals [32]. Three fuzzy membership functions: N (negative), Z (zero), and P (positive) are assigned to each input. The membership functions are triangular and equally distributed, as seen in Figure 5. Equally distributed triangle membership functions are more effective for the controller, especially in this case, according to the author's testing of unequally distributed membership functions concentrated inside a certain interval, as described in [33]. Based on the expected maximum and minimum values of the frequency deviation and its derivative, the membership function ranges are selected.

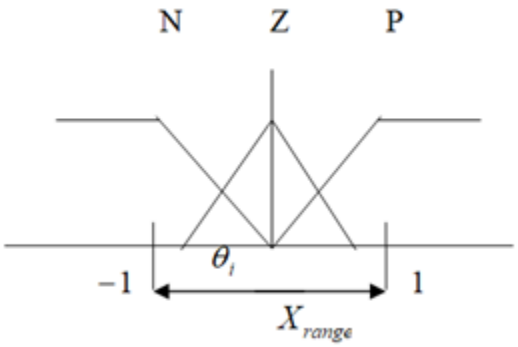


Figure 6: The membership functions used for the ARFLFC inputs variables [34]

B. Step 2

Develop a rule base for the fuzzy basis function (FBF) using two inputs ΔP and Δ$P$, and one output. As shown in Table 2, set the starting value of the parameter vector $\theta$ as the initial fuzzy rule base. This value is chosen based on the designer's expertise and the table look-up scheme proposed in [35]. Apply the adaptation law (33) to compute the estimated parameter vector $\theta$ online, as shown in Table 3. Then, calculate the FBF from equation (15) and apply the results to equation (34) to obtain the load frequency control (LFC) output.

C. Step 3

To obtain the gains of controller error, $k$, use trial and error.

TABLE 2. Initial fuzzy rule base of ARFLFC

| ΔP / Δ$\dot{P}$ | N | Z | P |
|---|---|---|---|
| N | N | N | Z |
| Z | N | Z | P |
| P | Z | P | P |

*International Journal of Engineering Applied Sciences and Technology, 2024*
**Vol. 9, Issue 06, ISSN No. 2455-2143, Pages 14-24**
**Published Online October 2024 in IJEAST (http://www.ijeast.com)**

TABLE 3. Tunable fuzzy rule base of ARFLFC

| $\Delta P$ / $\dot{\Delta P}$ | $N$ | $Z$ | $P$ |
|---|---|---|---|
| $N$ | $\hat{\theta}_1$ | $\hat{\theta}_2$ | $\hat{\theta}_3$ |
| $Z$ | $\hat{\theta}_4$ | $\hat{\theta}_5$ | $\hat{\theta}_6$ |
| $P$ | $\hat{\theta}_7$ | $\hat{\theta}_8$ | $\hat{\theta}_9$ |

## VII. SIMULATIONS RESULTS

In this study, a comparative analysis was conducted between an integral controller and the proposed Adaptive Fuzzy Logic Load Frequency Control (ARFLFC). Time-domain simulations of the two power areas were carried out using Matlab/Simulink, with detailed system parameters provided in Table 4. Area 1 had a 0.187 per unit (pu) positive load disruption Figures 6 and 7, respectively, showed the frequency deviations' dynamic responses for area 1 (Δf1) and area 2 (Δf2). The simulations revealed effective frequency deviation management for each area.

Table 4. Parameters of the two power area.

| Parameters | Area1 | Area2 |
|---|---|---|
| Speed regulation –$R$ | $R_1 = 0.05$ | $R_2 = 0.0625$ |
| Frequency sensitive load coefficient –$D$ | $D_1 = 0.6$ | $D_2 = 0.9$ |
| Inertia constant –$H$ | $H_1 = 5$ | $H_2 = 4$ |
| Governor time constant - τG | $\tau_{G1} = 0.2\ s$ | $\tau_{G2} = 0.3\ s$ |
| Turbine time constant - τT | $\tau_{T1} = 0.5\ s$ | $\tau_{T2} = 0.6\ s$ |
| Synchronizing coefficient –$T_{12}$ | $T_{12} = 2\ pu$ | |

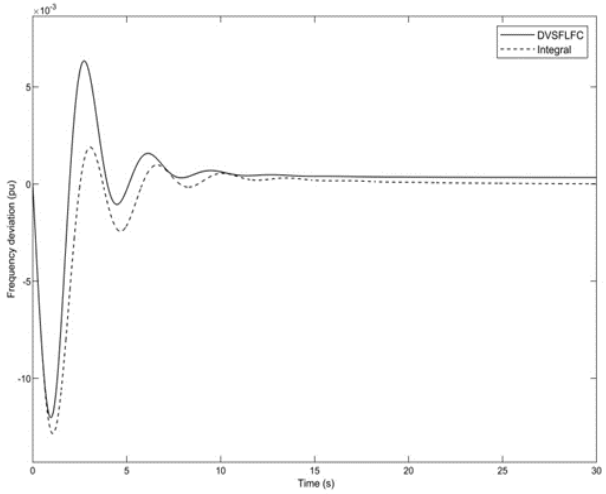


Figure 7: Frequency deviation in area-1.

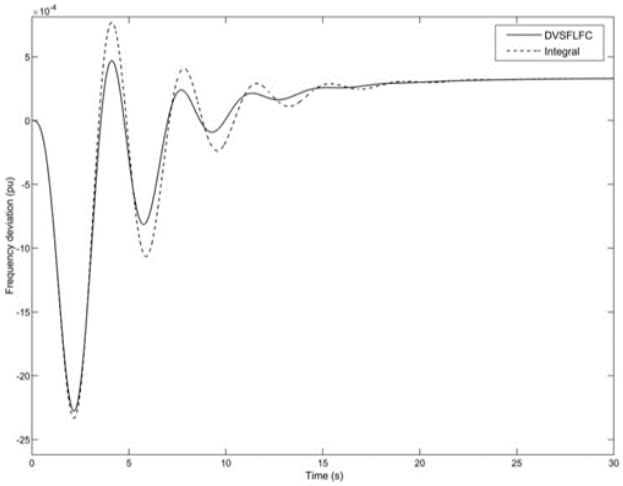


Figure 8: Frequency deviation in area-2.

The steady-state tie-line power deviation approached zero for the ARFLFC and integral controller setups, as shown in Figures 9, 10, and 11.

*International Journal of Engineering Applied Sciences and Technology, 2024*
**Vol. 9, Issue 06, ISSN No. 2455-2143, Pages 14-24**
**Published Online October 2024 in IJEAST (http://www.ijeast.com)**

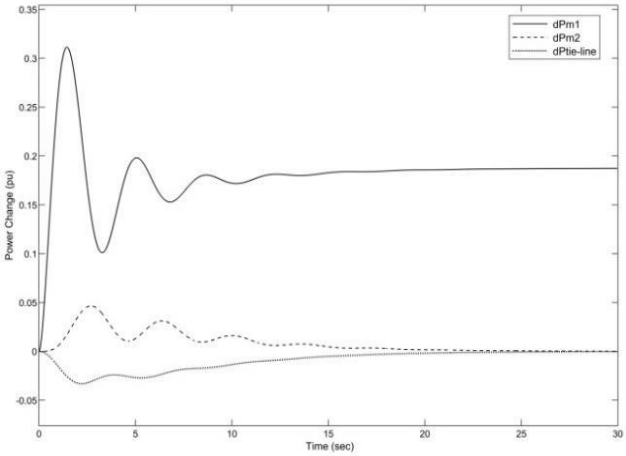


Figure 9: power deviations for integral controller.

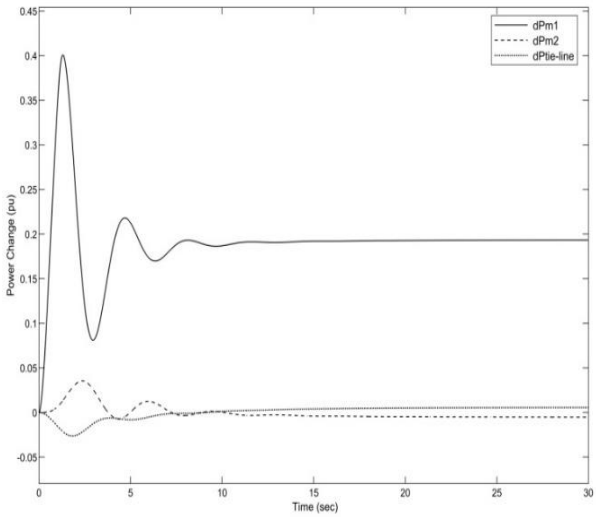


Figure 10: power deviations for ARFLFC controller.

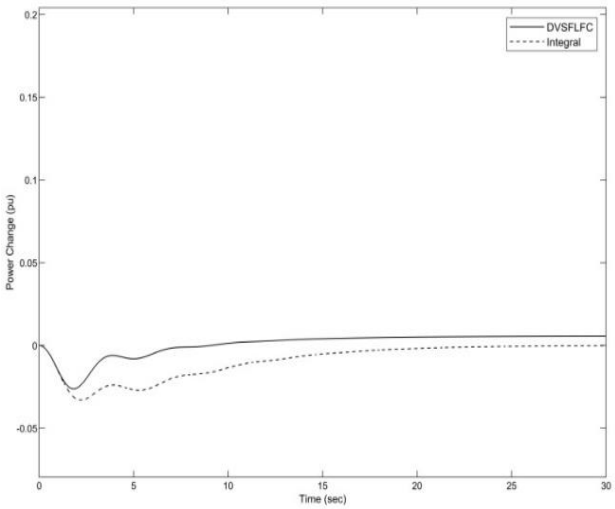


Figure 11: Tie-line power deviations between areas.

The mechanical power responses depicted in Figures 12–13 showcased each area's ability to handle its own load disturbances, maintaining operational independence between areas.

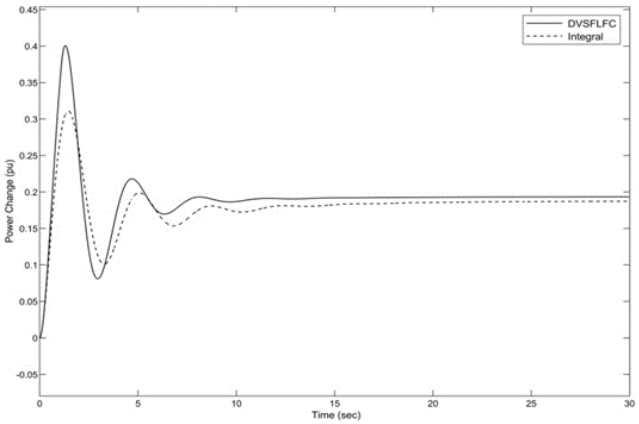


Figure 12: Mechanical power deviations in area-1.

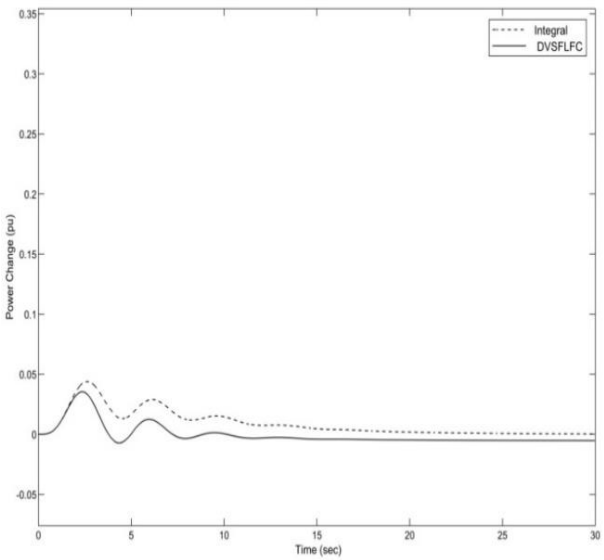


Figure 13: Mechanical power deviations in area-2.

The comparative analysis of the performance index, represented by $Jp = \Sigma\Delta\omega_2$, in Table 3 highlighted the superior performance of ARFLFC over the integral control. Due to the non-linear nature of ARFLFC, it exhibited more consistent management of non-linear behaviors across different operating conditions compared to the linear integral controller. ARFLFC's adaptability ensured proper response to system dynamics and changes, surpassing the inflexibility of traditional controllers in maintaining system stability and meeting output requirements in varying conditions. The simulation tests confirmed the effectiveness of ARFLFC in enhancing power system dynamic responses and achieving load frequency control (LFC) goals even in the presence of parameter uncertainties, positioning ARFLFC as a robust and efficient controller in power

system control.

Table 5. $Jp$ performance index of frequency deviations for ARFLFC and Integral controller.

| ARFLFC Controller | | Integral Controller | |
|---|---|---|---|
| Area 1 | Area 2 | Area 1 | Area 2 |
| 8.25 | 4.9 * 10-3 | 10.45 | 6.9 * 10-3 |

## VIII. CONCLUSION

This work introduced the load frequency controller for a multi-area power system with unknown parameters, utilizing the direct variable structure adaptive fuzzy logic (ARFLFC) technique. An adaptation algorithm based on the Lyapunov direct technique was developed to guide the system towards a desired response. Through trial and error, it was possible to fine-tune the controller's gains to minimize frequency deviations. Simulation results

## IX. REFERENCES

[1]. M. N. M. Jamadar and M. A. R. Reddy, "Load Frequency Control for Two Area Deregulated Power System Using ANN Control," 2015.

[2]. D. G. Padhan and S. J. I. t. Majhi, "A new control scheme for PID load frequency controller of single-area and multi-area power systems," vol. 52, no. 2, pp. 242-251, 2013.

[3]. A. Morinec and F. Villaseca, "Continuous-mode automatic generation control of a three-area power system," in The 33rd North American Control Symposium, 2001, pp. 63-70.

[4]. M. A. Faraj, S. K. Mousa, H. S. Mussa, A. A. Abdullah, A. Q. Mousay, and E. M. Jummah, "Using Optimization Technique for Optimal Tuning PID Controller in Multi-Area Automatic LFC," 2021.

[5]. A. J. F. C. Darwish and I. Journal, "Bio-inspired computing: Algorithms review, deep analysis, and the scope of applications," Future Computing and Informatics Journal, vol. 3, no. 2, pp. 231- 246, 2018.

[6]. S. Sinha, R. Patel, R. J. I. J. o. C. T. Prasad, and Engineering, "Application of GA and PSO tuned fuzzy controller for AGC of three area thermal thermal-hydro power system," vol. 2, no. 2, p. 238, 2010.

[7]. ] B. Mohanty, S. Panda, P. J. I. j. o. e. p. Hota, and e. systems, "Controller parameters tuning of differential evolution algorithm and its application to load frequency control of multi source power system," vol. 54, pp. 77-85, 2014.

[8]. G. Chen, Z. Li, Z. Zhang, and S. J. I. A. Li, "An improved ACO algorithm optimized fuzzy PID controller for load frequency control in multi area interconnected power systems," vol. 8, pp. 6429-6447, 2019.

[9]. E. Sahin, "Design of an optimized fractional high order differential feedback controller for load frequency control of a multi-area multi-source power system with nonlinearity," IEEE Access, vol. 8, pp. 12327-12342, 2020.

[10]. M. T. Alrifai, M. F. Hassan, M. J. I. J. o. E. P. Zribi, and E. Systems, "Decentralized load frequency controller for a multi-area interconnected power system," vol. 33, no. 2, pp. 198-209, 2011.

[11]. K. Sudha, R. V. J. I. J. o. E. P. Santhi, and E. Systems, "Load frequency control of an interconnected reheat thermal system using type 2 fuzzy system including SMES units," vol. 43, no. 1, pp. 1383-1392, 2012.

[12]. T. Hussein and A. J. D. Shamekh, "Design of PI fuzzy logic gain scheduling load frequency control in two-area power systems," vol. 3, no. 2, p. 26, 2019.

[13]. H. Benbouhenni, Z. Boudjema, and A. J. I. J. o. S. G. Belaidi, "Using three-level Fuzzy space vector modulation method to improve indirect vector control strategy of a DFIG based wind energy conversion systems," vol. 2, no. 3, pp. 155-171, 2018.

[14]. V. Utkin, J. Guldner, and J. Shi, Sliding mode control in electro-mechanical systems. CRC press, 2017.

[15]. A. Yesil, "Enhancing System Performance Using Fuzzy Scheduling Techniques for PI Controllers," International Conference on Fuzzy Systems, pp. 234-245, 2015.

[16]. P. Sharma, "Adaptive Fuzzy Scheduling Algorithms for PLD and Traditional PI Controllers," Journal of Control Engineering, pp. 112-125, 2017.

[17]. S. D. Al-Majidi, M. Kh. AL-Nussairi, A. J. Mohammed, A. M. Dakhil, M. F. Abbod, and H. S. Al-Raweshidy, "Design of a load frequency controller based on an optimal neural network," Energies, vol. 15, no. 17, p. 6223, 2022.

[18]. P. J. P. s. s. Kundur and control, "Power system stability," vol. 10, pp. 7-1, 2007.

[19]. D. J. I. J. o. E. Sharma, Science and Technology, "Automatic generation control of multi source interconnected power system using adaptive neuro-fuzzy inference system," vol. 12, no. 3, pp. 66-80, 2020.

[20]. Y. Wang, R. Zhou, and C. Wen, "Robust load frequency controller design for power systems," in IEE proceedings C (generation, transmission and distribution), 1993, vol. 140, no. 1, pp. 11- 16: IET.

[21]. N. Jaleeli, L. S. VanSlyck, D. N. Ewart, L. H. Fink, and A. G. J. I. t. o. p. s. Hoffmann, "Understanding automatic generation control," vol. 7, no. 3, pp. 1106-1122, 1992.

[22]. H. Hagras, V. Callaghan, M. Colley, and G. J. I. S. Clarke, "A hierarchical fuzzy–genetic multi agent architecture for intelligent buildings online learning, adaptation and control," vol. 150, no. 1-2, pp. 33-57, 2003.

[23]. R. S. H. Al-Joubori, "Tuning of Fuzzy Logic Controller Using Genetic Algorithms," 2001.

[24]. M. A. E. Mohamed, F. M. A. Bendary, K. A. M. El-Metwally, and W. M. M. Ibrahim, "Fuzzy stabilizer design for renewable energy based distribution networks," in 22nd International Conference and Exhibition on Electricity Distribution (CIRED 2013), 2013, pp. 1-4: IET.

[25]. K. El-Metwally, "An adaptive fuzzy logic controller for a two area load frequency control problem," in 2008 12th International Middle East Power System Conference, 2008, pp. 300- 306: IEEE.

[26]. W. Farag, H. El-Hosary, K. El-Metwally, A. J. J. o. I. Kamel, and F. Systems, "Design and implementation of a variable-structure adaptive fuzzy-logic yaw controller for large wind turbines," vol. 30, no. 5, pp. 2773-2785, 2016.

[27]. L.-X. Wang, A course in fuzzy systems and control. Prentice-Hall, Inc., 1996.

[28]. L.-X. Wang, Adaptive fuzzy systems and control: design and stability analysis. Prentice-Hall, Inc., 1994.

[29]. S. Pothiya, I. Ngamroo, S. Runggeratigul, P. J. I. J. o. C. Tantaswadi, Automation,, and Systems, "Design of optimal fuzzy logic based PI controller using multiple tabu search algorithm for load frequency control," vol. 4, no. 2, pp. 155- 164, 2006.

[30]. A.-L. Elshafei, K. El-Metwally, and A. J. C. E. P. Shaltout, "A variable-structure adaptive fuzzy logic stabilizer for single and multi-machine power systems," vol. 13, no. 4, pp. 413-423, 2005.

[31]. L. Hsu, A. D. de Araújo, and R. R. J. I. t. o. a. c. Costa, "Analysis and design of I/O based variable structure adaptive control," vol. 39, no. 1, pp. 4-21, 1994.

[32]. J. A. Momoh, X. W. Ma, and K. J. I. T. o. p. s. Tomsovic, "Overview and literature survey of fuzzy set theory in power systems," vol. 10, no. 3, pp. 1676-1690, 1995.

[33]. H. Zhuang, X. J. I. T. o. S. Wu, Man,, and P. B. Cybernetics, "Membership function modification of fuzzy logic controllers with histogram equalization," vol. 31, no. 1, pp. 125-132, 2001.

[34]. T. Hussein and A. Shamekh, "Adaptive rule-base fuzzy power system stabilizer for a multi machine system," in 21st Mediterranean Conference on Control and Automation, 2013, pp. 1514-1519: IEEE.

[35]. L.-X. Wang and C. J. I. t. o. f. s. Wei, "Approximation accuracy of some neuro-fuzzy approaches," vol. 8, no. 4, pp. 470-478, 2000.